ANNALS OF GEOPHYSICS, 53, 4, 2010; doi: 10.4401/ag-4683

RESEARCH ARTICLES

Preliminary outline of the seismologically active zones in Syria

Mohamad Khir Abdul-Wahed[1,*] and Ibrahim Al-Tahhan[2]

[1] *Atomic Energy Commission of Syria (AECS), Department of Geology, Damascus, Syria*

[2] *General Establishment of Geology and Mineral Resources, Damascus, Syria*

Article history
Received April 7, 2010; accepted July 16, 2010.
Subject classification:
Seismotectonics, Faulting, Fault-plane solutions, Focal mechanism, Syria, Dead Sea fault system.

ABSTRACT

The aim of this study was to outline the seismologically active zones in Syria using the focal mechanisms of the largest events recorded by the Syrian National Seismological Network over the last decade. A dataset of fault-plane solutions was obtained for 49 events with magnitude ≥3.5 using the first P-wave motions. Most of these events had strike–slip mechanisms in agreement with the configuration of the seismogenic belts in Syria. Normal mechanisms were more scarce and were restricted to certain areas, such as the coastal ranges. These data show that despite the relatively small magnitudes of the events studied, they provide a coherent picture of the deformation that has currently been taking place along the active faults. However, some other faults were inactive during the period of this study.

Introduction

Syria is located in the northern part of the Arabian plate (Figure 1). It is bound in the West by the northern section of the Dead Sea Fault System (DSFS). North-East of Antioch, the DSFS intersects the Eastern Anatolian Fault System (EAFS) and the Bitlis Suture zone, both of which comprise the northern border of the Arabian plate. Between Damascus and the Euphrates River, the NE trending of the Palmyra fold–thrust belt is located within the northern Arabian plate [Dubertret 1966, Ponikarov 1966]. It has been shown that the tectonic deformation within Syria [e.g. Barazangi et al. 1993] has been controlled by repeated collisions, openings and movements at the plate boundaries that almost completely surround Syria (Figure 1). The neotectonic map of Syria recently published by Rukieh et al. [2005] illustrated the evolution of the north-western boundary zone of the Arabian plate. Previous studies on the focal mechanisms of the past events in Syria have illustrated the left-lateral pattern of active deformation, with minor components of normal faulting associated with pull-apart basins along the DSFS [Garfunkel et al. 1981, Chaimov et al. 1990, Barazangi et al. 1993]. Salamon et al. [2003] calculated the fault-plane mechanisms of all $M_L \geq 4$ seismicity recorded in the eastern Mediterranean region during the 20th century. They found anomalous solutions that attest to the complexity of the deformation processes along the DSFS.

The Syrian National Seismological Network (SNSN) was installed and has been operated since January 14, 1995 [Dakkak et al. 2005]. This network consists of 27 short-period (1 Hz) stations, and it has provided 10 years of local instrumental data for the first time in Syria. The design objective of the SNSN was to monitor all of the discernible earthquake activity along the DSFS and its related branches in Syria and in nearby Lebanon (Figure 2).

The seismicity of Syria and the adjacent areas over the last century can be classified as moderate. The main instrumental seismicity with many moderate earthquakes ($5 < M_S < 6$) is located along the EAFS and the DSFS [Sbeinati 1993]. The purpose of this study was to outline the focal mechanisms of the largest events ($M_L > 3.5$) recorded by the SNSN over the last ten years. These data are described as preliminary because the return periods of large earthquakes ($M \geq 5$) in Syria are long. These were estimated by Ambraseys and Barazangi [1989] at about 200-350 years. Therefore, some of the faults, such as the Damascus Fault (South-West Palmyra region), appeared to be seismological inactive during the period of this study. A longer study will further define the seismicity in Syria. Thus, we have focused in the present study on the mechanisms of the only 49 selected events that were recorded by the SNSN; these are relatively suitable for computing and can be compared with the main faults in Syria.

Methods

A probabilistic method was used, as proposed by Zollo and Bernard [1991]. This is a non-linear inversion method for studying earthquake mechanisms. Assuming a double-couple, point-source model and a well-determined earthquake location, the model parameters are the fault angle orientations [strike, dip and slip (or rake)] [Aki and Richards 1980]. The probability of parameters (strike, dip and slip fault angles) for the given observational dataset, the

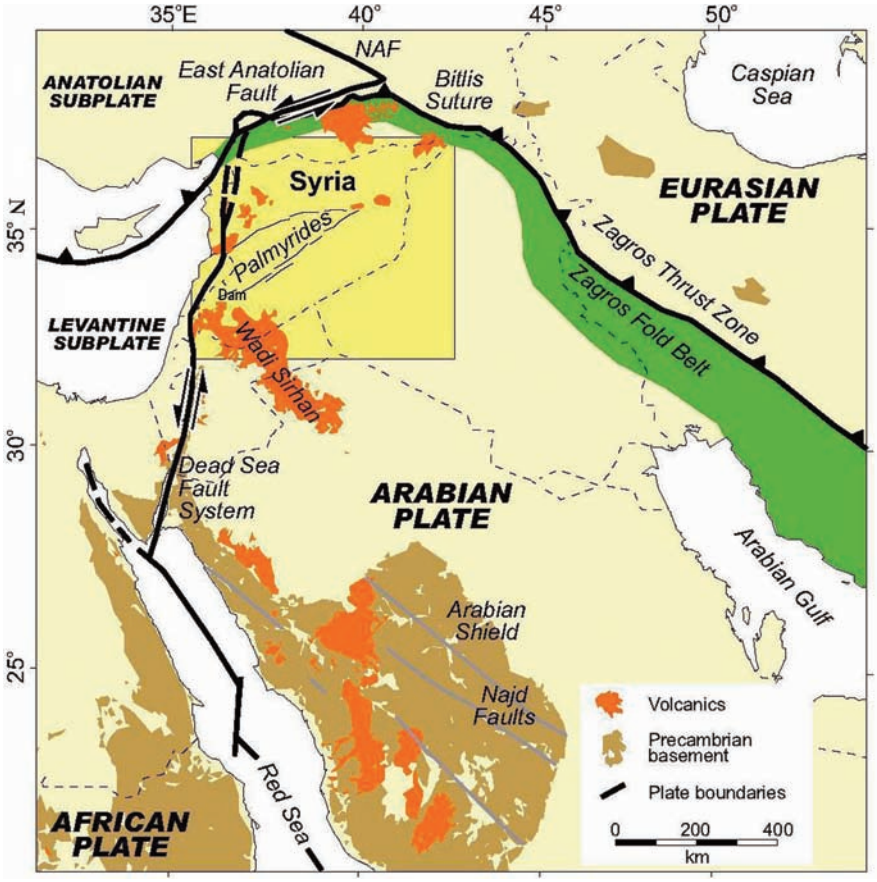

Figure 1. Regional tectonic map of the northern Arabian Plate and the surrounding regions, showing the proximity of Syria to many active plate boundaries. Dam, Damascus; NAF, North Anatolian Fault (modified from Brew et al. 2001). The yellow square shows the area in Figures 2, 3, 4 and 5.

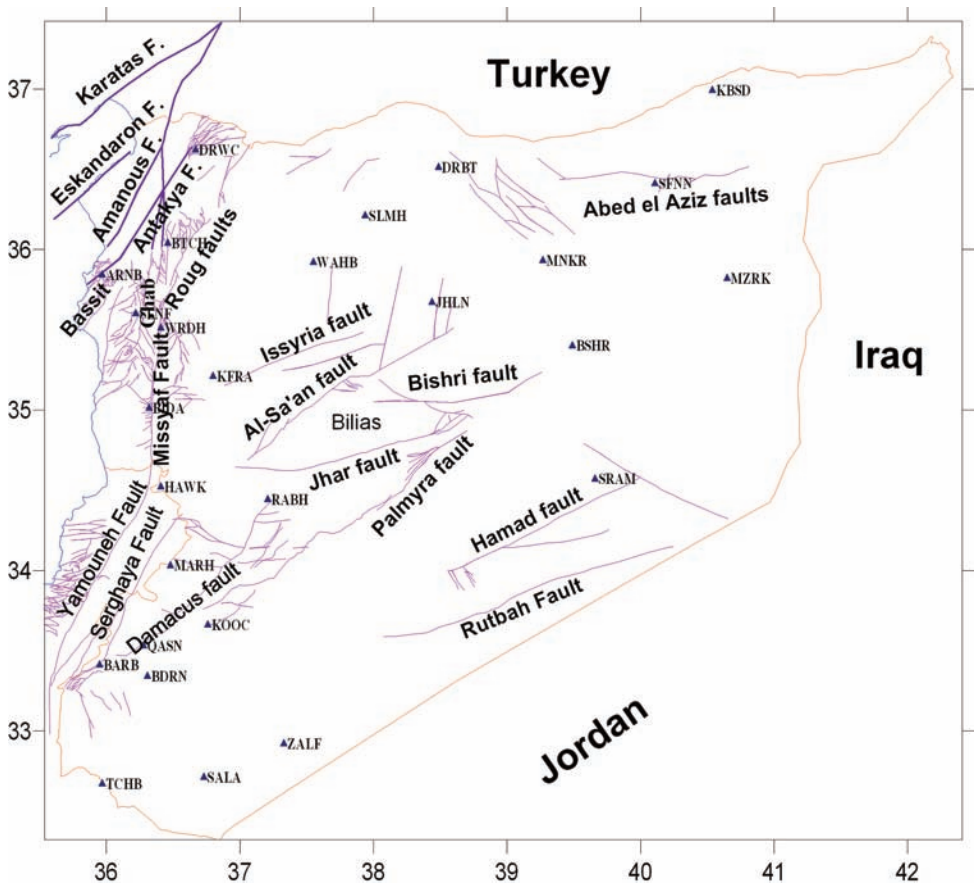

Figure 2. Map of the geographical distribution of the Syrian National Seismological Network (▲) and the principal faults in this area.

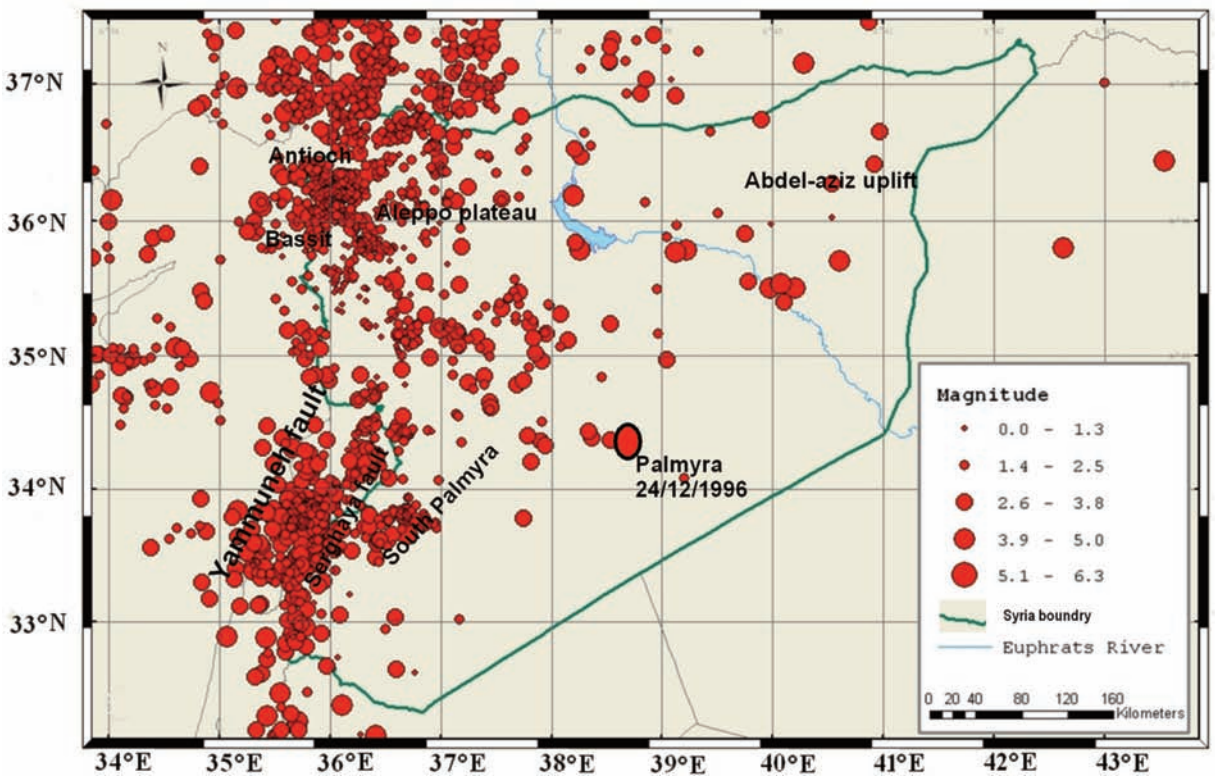

Figure 3. Earthquake activity in Syria and its nearby regions, as documented by the Syrian National Seismological Network from 1995 to 2004 (modified from Alchalbi 2004).

P-wave polarities, were computed using a Bayesian approach. The *P*-wave polarity information is taken into account in the form of a prior probability density function, which was defined according to Brillinger et al. [1980]. The method was based on estimation through an exhaustive search of the probability of the model parameters. The maximum-likelihood solutions are only represented by their lower hemisphere projection in this study. Finally, it should be noted that in this study we were more concerned about the applications of the methodology, rather than the development of the method itself.

The seismicity of Syria over the last ten years

The SNSN has recorded about 1,200 local events since January 1995. More information about the SNSN data, such as acquisition, transmission, processing and recording can be found in Dakkak et al. [2005]. The seismicity of Syria can be classified as small-to-moderate magnitude during this period, as it had been over the previous century (Figure 3). The main instrumental seismicity with many moderate earthquakes ($5 < M_S < 6$) is located along the East Anatolian Fault and the northern extension of the DSFS, and especially in Lebanon. The seismicity inside Syria was characterized by many sets of weak events ($M_L < 4$) that were observed for the South Palmyra region, the Serghaya Fault, the South and West Aleppo plateau, the Bassit region and the coastal ranges (Figure 3). The most important event was an earthquake in the Palmyra region, which occurred on December 24, 1996, with magnitude of about 5.2.

Data quality

The low seismicity in Syria and the insufficient cover provided by the seismic stations of the SNSN until 2002 [Dakkak et al. 2005] limited the number of fault-plane solutions that can be obtained in Syria. We therefore carefully examined the available data and the reliability of the solutions, to get the most information out of them. Since the majority of the seismic events recorded in Syria were weak events ($M_L < 4$), all of the local events with magnitudes >3.5 were considered as main events in this study. Accordingly, 49 events inside Syria and in nearby regions were selected as the main events for the first motion analysis. The majority of these were recorded by 13 stations, on average. The accuracy of the location was a critical factor for the reliable identification of the faulting parameters. To improve the accuracy of the selected events, the records were filtered using a Butterworth order 3 filter, to obtain the best signal-to-noise ratio, and all of the *P* phases and *S* phases were manually picked. As a result, the number of arrival-time readings was increased. The locations were calculated again with the new arrival times using the same velocity model used by the SNSN. The Syrian velocity–depth model is based on data from seismic reflection and refraction surveys carried out in Syria [Preliminary Seismological Bulletin 1995]. This model is composed of a typical continental type of crust, with a thickness of about 38 km, and a normal mantle with a *P*-velocity of 8.0 to 8.2 km/s. The locations provided the ray angle orientations (azimuth, take-off according to Aki and Richards [1980]). Figure 4

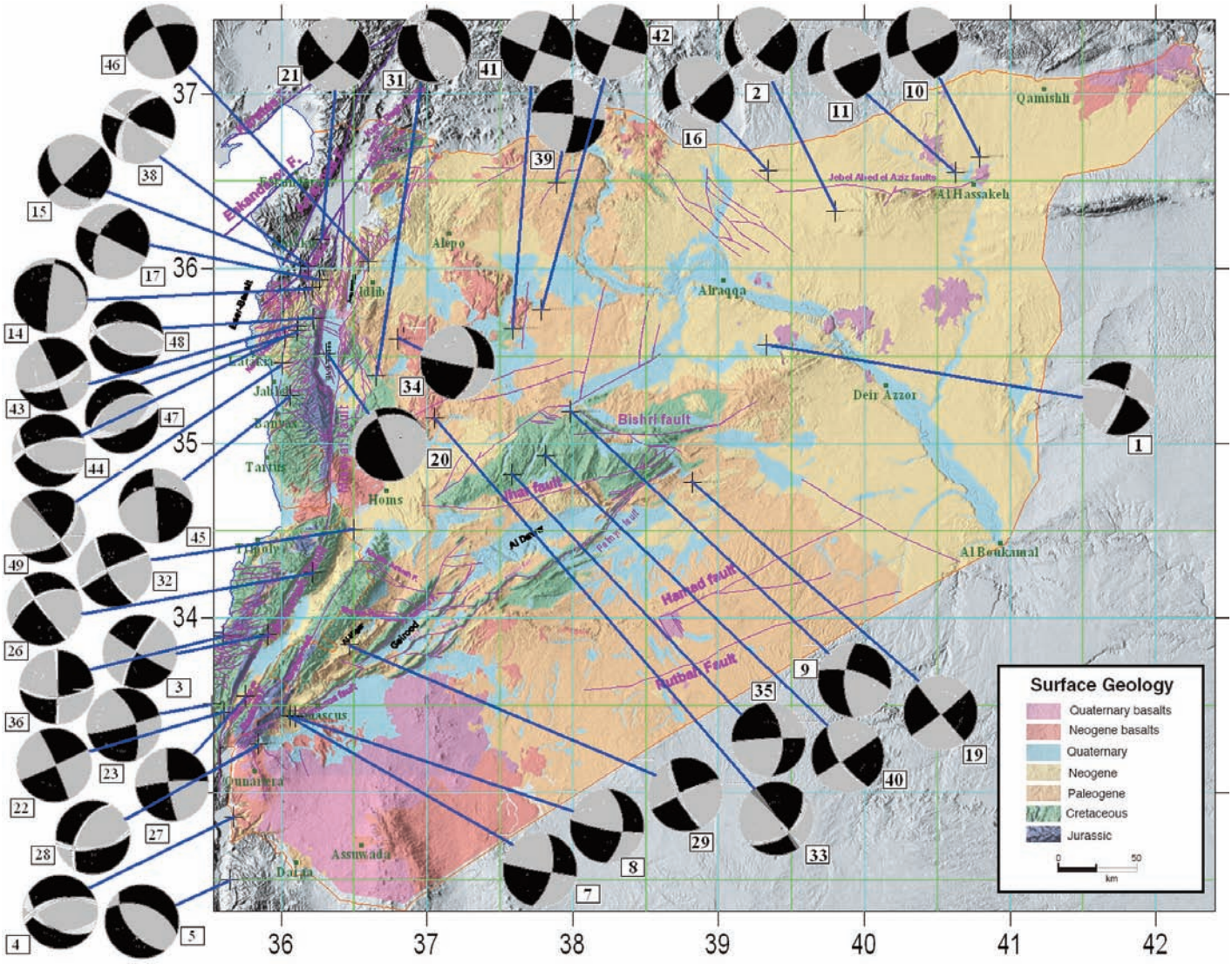

Figure 4. The focal mechanisms of the main events recorded over the last ten years in Syria and its nearby regions. The adjacent numbers indicate the event numbers in Appendix 1. The fault plane solutions are presented with lower-hemisphere, equal-area projections: white quadrants for dilatation, and black for compression. The base map showing the surface geology was modified by Brew et al. [2001], from Dubertret [1955], Ponikarov [1966] and Devyatkin et al. [1997].

shows the epicenter distribution of the earthquakes that were selected for the source mechanisms study.

Reliability of solutions

Using a Quality Factor (QF) is important for the evaluation of the data and their solutions, particularly because we mainly dealt with solutions that are based on few data. This QF is established in this study by the sum of many criteria known in the literature, with the criteria used to define QF as follows:

a) the degree to which the solutions fit the data (0, complete misfit; 1, poor fit; 2, fair fit; 3, good fit);

b) the azimuthal distribution of the data on the focal sphere or on the lower-hemisphere, equal-area projection (0, in one quadrant; 1, in two quadrants; 2, in three quadrants; 3, in four quadrants);

c) the homogeneity of distribution of the data on the focal sphere or on the lower-hemisphere, equal-area projection. The more widely the data are spread, the better the focal sphere is represented (0, concentrated; 1, poor spread; 2, fair spread; 3, good spread);

d) The total number of polarities used for construction of the focal plane solutions (0, <10; 1, 10-15 (poor); 2, 15-20 (fair); 3, >20 (good)).

e) the number of reversed polarities. As the number increases, the reliability decreases (0, >30%; 1, 20%-30%; 2, 10%-20%; 3, <10%).

The sum of these points then defines the QF as the reliability of a solution. The higher the QF, the better the reliability of a solution. The maximum QF can reach is 15. Appendix 1 shows the reliability (QF) of the calculated fault plane solutions using the above criteria.

Results

The probabilistic method proposed by Zollo and Bernard [1991] was applied to the selected events. Most of these had strike–slip mechanisms in agreement with the nearby local fault structures. Normal mechanisms were

scarce (seen for only 6 events), and they were restricted to certain areas, such as the coastal ranges. No reverse mechanisms were observed. The patterns of seismicity for the largest events recorded in Syria over the last decade are presented in Figure 4. This is consistent with the configurations of the main seismogenic belts in Syria. The mechanisms calculated will be described in the following sections. Appendix 2 shows some examples of the *P* first motion plots, from which the focal mechanisms of Figure 4 were derived, and the data used in the probabilistic method (ray angle orientations, *P* polarity).

Discussion

The study area covered two major tectonic domains: the DSFS and the intersection of the DSFS with the EAFS, to the North-East of Antioch. Some events were located inside Syria on other fault systems.

The Dead Sea Fault System

The DSFS and its related branches, including the Serghaya Fault in Syria and the Yammuneh and Roum Faults in Lebanon, have been characterized by sinistral strike–slip motions. The principal left lateral sense motion of the DSFS has been recognized by minor pull-apart in young sediments [Garfunkel et al. 1981, Trifonov 1991, Brew et al. 2001], the cut and offset of drainage lines, and man-made structures [Brew et al. 2001, Gomez et al. 2001, Gomez et al. 2003, Meghraoui et al. 2003, Gomez et al. 2006]. The current seismicity associated with the DSFS supports these findings, and is concentrated along the southern part of the DSFS [Salamon et al. 2003]. Albeit that most of the mechanisms that it was possible to compute were from small events, their variety provided valuable insights into the complexity of the DSFS and the structures along it. Good agreement was seen between the fault-plane solutions of events 7 and 8 in Figure 4, which occurred on November 22, 1995, and the NE Serghaya Fault. Also, this was similar to the fault-plane solutions of events 22 and 23, which occurred on March 26, 1997, and the NW Roum Fault. These two faults branch out of the DSFS at the southern deflection point of the Yammouneh Bend. Thus, events 7, 8, 22 and 23 recorded left-lateral motion on NS-striking faults.

According to our observations, three events in the South-West of Syria (events 4, 5, 28) had a normal fault mechanism. They were probably related to the local structure and to the lateral motion along the DSFS. Event 5 can be related to local trans-tensional faults, and might be related to the Al-Sirhan Fault System. Salamon et al. [2003] found that the normal mechanisms of some events near the Dead Sea and the Gulf of Aqaba record the activities of normal faults that extend along the margins of the Dead Sea depression and other parts of the DSFS.

Event 3, which occurred North of Zahleh, showed dextral motion on the NS striking nodal plane. It might have been related to a probable mislocation, and it might also have been generated on the Yammouneh Fault itself. This might reflect distributed complex deformation near to the transform, such as was described by Salamon et al. [2003] and Ron and Eyal [1985]. This anomaly attests to the complexity of the deformation processes along the transform fault. The mechanism of event 36 can be related to a right-lateral EW striking fault in the North of Beirut. Two events, 32 and 26, had sinistral mechanisms trending NW and these can be related to the transform fault. One event (event 20) was located in the middle of the Al-Ghab Valley (a large pull-apart basin). This event had a normal mechanism, in agreement with the existing NW normal fault associated with local trans-tensional features [Trifonov 1991, Brew at al. 2001]. Normal mechanisms were also observed in the coastal range events, and these might be associated with local trans-tensional features.

Intersection of the DSFS with the EAFS

The second domain is the intersection of the DSFS with the EAFS (Figures 1, 3). The EAFS in Antioch is a NE sinistral strike–slip transform. The greatest magnitude occurred in this domain, and this was the earthquake of Antioch on January 22, 1997. This event, as event 21 in Figure 4, had a sinistral strike–slip mechanism trending NE, in agreement with the Antioch Fault (Figure 2, Antakia F). The three events 15, 17 and 38 showed the same focal mechanisms and were also observed along the Latakia-Kelles Faults in the Bassit region. In addition, one event that was noticed in the North of Jesser-Elshgour had a normal fault mechanism with a sinistral strike–slip component, trending NS. This event was probably related to the extensions in the DSFS margins. The DSFS also branched toward the North-East in the Al-Rouge Plain. Event 46 was located in this region, and it had a sinistral mechanism, trending NE, in agreement with the existing faults.

Inside Syria

Some events were observed for the Aleppo Plateau (Figure 3), such as the two events 31 and 34 in the South-West. Event 31 had a normal fault mechanism, in agreement with the NW existing fault. Another two events, as 41 and 42, that were located in the South-East of the Khanaser region, had a sinistral mechanism, trending NE. These might have been related to one of the existing N15E faults. Between the Aleppo Plateau and the Palmyra fold-thrust belt, the two events 9 and 33 had dextral mechanisms. The first of these was located on the Al-Sa'an Fault, while the second, event 33, was located in the South-East of Issyria, where the Bishri dextral fault separates the Bilas-Bishri blocs. Two events (35 and 40) were located inside the Bilas bloc and had a sinistral mechanism. The earthquake of Palmyra in 1996 had a

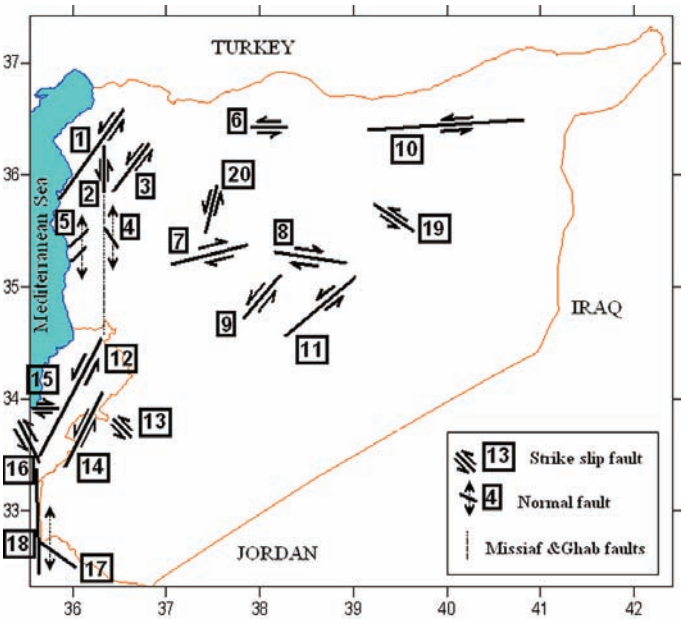

Figure 5. Simplified interpretation of the focal mechanisms over the last decade for the largest events in Syria. The active faults proposed to be generating these events were: 1, East Anatolian Fault System; 2, Northern section of the Dead Sea Transform System; 3, Rouge Faults; 4, Normal faults in the Al-Ghab pull-apart basin; 5, Normal faults in the coastal ranges; 6, Manbeg Fault; 7, Al-Sa'an Fault; 8, Dextral fault separating the Bilas-Bishri Blocs; 9, Bilas Bloc Faults; 10, Abdel-Aziz uplift Faults; 11, Palmyra Faults; 12, Yammouneh Fault; 13, Ma'alola Fault; 14, Serghaya Fault; 15, Dextral fault in the north of Beirut; 16, Roum Fault; 17, Normal faults on the margins of the DSFS; 18, The DSFS; 19, Bishri Faults; 20, Khanaser Fault.

sinistral mechanism trending NE. Event 1, which was located in the North-East of Al-Bishri Mountain, showed sinistral motion on the NW striking nodal plane; this event can be related to the subsurface faults mapped by Brew et al. [2001].

In the South-West of the Palmyra fold-thrust belt, event 29, which was located in the South-West of Ma'alola, had a sinistral mechanism, trending NW. Considering the probable mislocation, this event might be related to the left-lateral NW-striking fault. This fault separated the AboulAta and Soueika Mountains. It was seen that the NW-striking nodal plane is in agreement with this fault, but that the event was located away from this fault. In an examination of the historical data [Sbeinati et al. 2005] and the instrumental data (1900-1991), Sbeinati [1993] reported some historical earthquakes that had occurred to the South-West of Ma'alola, like the earthquake of November 24, 1705, of M_S 6.9, and the earthquake of April 05, 991, of M_S 7.1. So, event 29 can be related to an unidentified fault.

The four events 2, 10, 11 and 16 that were located in the North-East of Syria had a sinistral mechanism, trending EW. These events were located along the Abdel-Aziz uplift faults, and showed nearly identical left-lateral strike–slip mechanisms.

These details are illustrated schematically in Figure 5, according to which it can be deduced that there were many active faults in the region during the period of this study. These included the Palmyra Faults, the Yammouneh Fault, the Ma'alola Fault, the Serghaya Fault and the Bishri Faults. This appears to confirm what has been known about these faults for a long time. From the data obtained in the present study, it can be noted that many other faults did not appear to be seismologically active, even though they were previously classified as known active faults, such as the Damascus Fault, the Jhar Fault, and others.

Conclusion

In the present study, 49 events of $M \geq 3.5$ were selected as the largest events in Syria over last decade. According to the data obtained, it can be concluded that most of the events studied had strike–slip mechanisms that are in agreement with the configuration of the major seismogenic belts in Syria. The data also reveal that normal mechanisms were restricted to certain areas, such as the coastal ranges. The normal mechanisms observed in the South-West of Syria and in the coastal ranges might be related to the trans-tensional features along the margins of the Dead Sea Transform System. In addition, many faults in the region were active during the period of this study, including the Palmyra Faults, the Yammouneh Fault, the Ma'alola Fault, the Serghaya Fault, and the Bishri Faults.

These data are still preliminary, because the return periods of large earthquakes ($M \geq 5$) in Syria are quite long. Indeed, although some faults, such as the Damascus Fault, were seismologically inactive during this study period, they might be active over longer time periods. As the events studied have relatively small magnitudes, they provide a coherent picture of the deformation that has been taking place along the active faults throughout Syria over the last decade.

Acknowledgements. The authors wish to express their thanks to Prof. Ibrahim Othman, Director General of the Atomic Energy Commission of Syria, for his constant support. They also wish to thank the General Establishment of Geology and Mineral Resources for providing some important information and data.

References

Alchalbi, A., (2004). Workshop on «Earthquake Hazard Assessment in Syria and Lebanon. Progress results and future strategies», September 7-9, 2004, Damascus, Syria.

Aki, K., and P.G. Richards (1980). Quantitative Seismology, Theory and Methods, 1st edition, San Fransisco, 573 pp.

Ambraseys, N., and M. Barazangi (1989), The 1759 Earthquake in the Bekaa Valley: Implications for Earthquake Hazard Assessment in the Eastern Mediterranean Region, J. Geophys. Res., 94 (B4), 4007-4013.

Barazangi, M., D. Seber, T. Chaimov, J. Best and T. Sawaf (1993). Tectonic evolution of the northern Arabian plate in western Syria, in: E. Boschi, E. Mantovani and A. Morelli, (eds.), Recent Evolution and Seismicity of the Mediterranean Region, Kluwer Academic Publishers, NATO ASI Series, The Netherlands, 117-140.

Brew, G., M. Barazangi, A.K. Al-Maleh and T. Sawaf (2001). Tectonic and geologic evolution of Syria, GeoArabia, 6 (3), 573-616.

Brillinger, D.R., A. Udias and A. Bolt (1980). A probability model for regional focal mechanisme solutions, Bull. Seism. Soc. Am., 70 (1), 149-170.

Chaimov, T.A., M. Barazangi, D. Al-Saad, T. Sawaf and A. Gebran (1990). Crustal shortening in the Palmyride fold belt, Syria, and implications for movement along the Dead Sea fault system, Tectonics, 9, 1369-1386.

Dakkak, R., M. Daoud, M. Mreish and G. Hade (2005). The Syrian National Seismological Network (SNSN): Monitoring a major continental transform fault, Seismological Research Letters, 76 (4), 437-445; doi: 10.1785/gssrl.76.4.437.

Devyatkin, E.V., A.E. Dodonov, E.V. Sharkov, V.S. Zykin, A.N. Simakova, K. Khatib and H. Nseir (1997). The El-Ghab rift depression in Syria: its structure, stratigraphy, and history of development, Stratigraphy and Geological Correlation, 5 (4), 362-374.

Dubertret, L. (1966). Liban, Syrie et bordures des pays voisins: tableau stratigraphique avec cette carte géologique au millionième, Notes et Mémoires sur le Moyen-Orient, 8, 251-358.

Garfunkel, Z., Y. Zak and R. Freund (1981). Active faulting in the Dead Sea rift, Tectonophysics, 80 (1-4), 1-26; doi: 10.1016/0040-1951(81)90139-6.

Gomez, F., M. Meghraoui, A.N. Darkal, R. Sbeinati, R. Darawcheh, C. Tabet, M. Khawlie, M. Charabe, K. Khair and M. Barazangi (2001). Coseismic displacements along the Serghaya fault: an active branch of the Dead Sea Fault System in Syria and Lebanon, J. Geol. Soc. Lond., 158, 405-408.

Gomez, F., M. Meghraoui, A.N. Darkal, F. Hijazi, M. Mouty, Y. Suleiman, R. Sbeinati, R. Darawcheh, R. Al-Gazzi and M. Barazangi (2003). Holocene faulting and earthquake recurrence along the Serghaya branch of the Dead Sea Fault System in Syria and Lebanon, Geophys. J. Int., 153 (3), 658-674.

Gomez, F., M. Khawlie, C. Tabet, A.N. Darkal, K. Khair and M. Barazangi (2006). Late Cenozoic uplift along the northern Dead Sea transform in Lebanon and Syria, Erth and Planetry Science Letters, 241 (3-4), 913-931; doi: 10.1016/j.epsl.2005.10.029.

Meghraoui, M., F. Gomez, R. Sbeinati, J. Van der Woerd, M. Mouty, A.N. Darkal, Y. Radwan, I. Layyous, H. Al-Najjar, R. Darawcheh, F. Hijazi and M. Barazangi (2003). Evidence for 830 years of seismic quiescence from palaeoseismology, archaeo seismology and historical seismicity along the Dead Sea Fault System, Earth and Planetry Science Letters, 210 (1-2), 35-52; doi: 10.1016/S0012-821X(03)00144-4.

Ponikarov, V.P. (1966). The Geology of Syria. Explanatory Notes on the Geological Map of Syria, Scale 1:200,000, Ministry of Industry, Damascus, Syrian Arab Republic.

Preliminary Seismological Bulletin (1995), SNSN: Syrian National Seismological Network, General Establishment of Geology and Mineral Resources, Syria.

Ron, H., and Y. Eyal (1985). Intraplate deformation by block rotation and mesostructures along the Dead Sea transform, Tectonics, 4 (1), 85-105; doi: 10.1029/TC004i001p00085.

Rukieh, M., V.G. Trifonov, A.E. Dodonov, H. Minini, O. Ammar, T.P. Ivanova, T. Taza, A. Yusef, M. Al-Shara and Y. Jobaili (2005). Neotectonic map of Syria and some aspects of Late Cenozoic evolution of the northwestern boundary zone of the Arabian plate, Journal of Geodynamics, 40 (2-3), 235-256; doi:10.1016/j.jog.2005.07.016.

Salamon, A., A. Hofstetter, Z. Garfunkel and H. Ron (2003). Seismotectonics of the Sinai subplate: the eastern Mediterranean region, Geophys. J. Int., 155 (1), 149-173.

Sbeinati, M.R. (1993). Instrumental catalogue of earthquakes in Syria and adjacent areas from 1900 to 1993, Report of a scientific visit to The Abdus Salam International Centre for Theoretical Physics (ICTP), Trieste, Italy, unpublished.

Sbeinati, M.R., R. Darawcheh and M. Mouty (2005). The historical earthquakes of Syria: an analysis of large and moderate earthquakes from 1365 B.C. to 1900 A.D., Annals of Geophysics, 48 (3), 347-435.

Trifonov, V.G. (1991). Levent fault zone in the northwest Syria, Geotectonics, 25, 145-154.

Zollo, A., and P. Bernard (1991). Fault mechanisms from near-source data: joint inversion of S polarization and P polarities, Geophys. J. Int., 104, 441-451.

*Corresponding author: Mohamad Khir Abdul-Wahed,
Atomic Energy Commission of Syria (AECS), Department of Geology, Damascus, Syria; e-mail: cscientific@aec.org.syt.

Appendix 1

Parameters of the fault-plane solutions of the first *P*-wave arrivals calculated in this study and their quality factors (QF). Each event number corresponds to the map of Figure 4.

Ev. N°	Date	Time (h)	Lat. (°N)	Long. (°E)	Depth (km)	M_L	M_{ISC}	Fault plane solutions						Q (≤15)	Probable fault
								First plane			Second plane				
								Az.	Dip	Slip	Az.	Dip	Slip		
01	1994/12/18	16:38:17.4	35.56	39.33	03.8	5.0	5.0	031	90	−150	301	60	000	6	Al-Bishri
02	1995/04/22	14:35:46.8	36.33	39.80	03.8	4.3	3.2	141	45	−175	046	85	−050	8	Abdel-aziz
03	1995/04/26	10:00:33.7	33.91	35.90	03.8	4.4	–	211	80	−175	121	85	−010	10	Yammouneh
04	1995/05/08	19:08:07.3	32.86	35.67	03.8	3.4	–	256	55	−110	106	40	−065	8	margins of DSFS
05	1995/08/08	00:15:39.6	32.50	35.65	03.8	3.8	–	291	45	−110	141	50	−065	8	margins of DSFS
06	1995/08/23	08:09:51.8	35.64	35.17	53.8	4.3	–	116	90	−110	031	20	000	9	Latakia-Kelles
07	1995/11/22	09:15:03.4	33.44	36.06	16.6	3.5	–	011	55	000	101	90	−145	13	Serghaya (DSFS)
08	1995/11/22	09:15:33.9	33.44	36.10	03.6	3.3	–	001	45	−015	101	80	−135	12	Serghaya (DSFS)
09	1995/11/24	23:42:45.4	35.18	37.99	13.8	3.2	–	181	60	−030	286	65	−145	9	Al-Sa'an
10	1996/01/04	15:28:07.3	36.64	40.79	02.5	4.7	4.5	161	50	−175	066	85	−050	7	Abdel-aziz
11	1996/01/11	23:03:36.2	36.55	40.62	03.8	4.6	3.5	161	45	−180	071	90	−045	7	Abdel-aziz
12	1996/05/23	20:44:52.8	34.30	34.28	30.4	4.6	–	041	85	−150	306	55	−010	8	
13	1996/06/05	13:12:58.0	35.79	35.70	03.7	4.5	4.5	076	55	−005	176	80	−130	7	Latakia-Kelles
14	1996/06/18	23:43:50.2	35.89	36.22	03.8	4.5	4.4	186	85	−080	296	10	−160	11	DSFS
15	1996/06/19	00:17:07.9	36.02	36.13	61.7	4.8	4.7	136	40	−180	046	90	−500	11	Latakia-Kelles
16	1996/07/09	21:49:22.1	36.56	39.34	03.8	4.8	3.9	146	45	−170	051	85	−045	9	Abdel-aziz
17	1996/07/19	17:54:04.3	35.93	36.26	03.6	3.9	–	296	90	−135	206	45	000	11	Latakia-Kelles
18	1996/12/03	22:13:00.0	33.27	35.34	03.8	3.3	–	196	90	−025	286	65	−180	9	Yammouneh
19	1996/12/24	22:16:19.7	34.78	38.82	03.2	5.7	5.2	046	80	−005	136	85	−170	9	Palmyra
20	1997/01/03	22:45:11.1	35.52	36.31	15.5	3.7	–	156	90	−075	246	15	−180	10	Al-Ghab
21	1997/01/22	17:57:06.5	36.17	36.27	08.3	5.7	5.6	041	70	−015	136	75	−165	12	Antioch
22	1997/03/26	04:22:35.3	33.41	35.40	04.4	5.4	5.6	076	85	−155	341	55	−010	8	Roum (DSFS)
23	1997/03/26	13:20:02.6	33.46	35.61	03.8	5.3	5.2	066	90	−175	336	85	000	9	Roum (DSFS)
24	1997/10/30	17:33:45.0	34.73	35.02	08.2	4.7	4.2	136	90	−150	046	60	000	8	Banyas
25	1997/12/14	03:11:02.2	34.97	34.87	34.0	4.1	–	116	85	−155	026	70	−010	8	Banyas
26	1998/02/05	22:49:53.0	34.26	36.21	06.8	3.9	–	241	50	−170	141	80	−045	12	Yammouneh
27	1998/02/13	19:10:05.3	33.55	35.75	03.8	3.9	–	171	80	−010	266	85	−170	10	Yammouneh
28	1998/02/25	03:35:15.8	33.28	35.84	03.8	3.2	–	206	50	−135	081	55	−050	10	margins of DSFS
29	1998/09/01	04:31:20.8	33.85	36.47	03.8	3.7	–	256	65	−155	151	65	−025	9	Ma'alola
30	1999/02/08	09:13:58.0	33.50	35.14	17.6	4.0	–	341	45	000	296	90	−135	11	
31	1999/04/07	07:44:35.2	35.38	36.65	03.8	4.1	–	306	40	−120	161	55	−070	10	Asharneh
32	1999/06/26	06:33:50.1	34.51	36.50	02.3	3.4	–	151	70	−010	241	80	−160	13	Yammouneh
33	2000/01/18	08:56:20.4	35.15	37.05	03.8	3.7	–	321	90	−050	051	40	−180	11	Al-Sa'an
34	2000/02/06	04:27:35.6	35.60	36.80	03.4	4.6	–	006	35	−005	101	85	−125	12	
35	2000/07/10	23:35:44.0	34.82	37.58	03.8	3.7	–	266	90	−040	356	50	−180	13	Bilas
36	2000/08/27	06:47:11.7	33.90	35.60	07.7	4.1	–	086	60	−180	356	90	−030	12	Beirut
37	2001/01/17	12:09:01.3	37.59	37.14	01.3	5.3	4.8	196	70	−130	091	55	−025	7	Amanous
38	2001/04/11	08:26:30.2	36.02	36.19	02.6	4.1	–	206	45	000	296	90	−135	11	Latakia-Kelles
39	2001/07/05	17:48:32.3	36.49	37.89	03.8	4.3	–	276	85	−010	006	75	−175	12	Menbeg
40	2002/06/10	10:05:45.3	34.93	37.81	05.6	4.1	–	146	65	−175	056	90	−025	11	Bilas
41	2002/09/08	19:57:15.3	35.66	37.59	07.0	5.4	4.8	111	85	−175	021	85	−005	10	Khanaser
42	2002/09/09	12:14:04.5	35.76	37.78	10.6	3.9	–	021	90	−010	111	80	−180	10	Khanaser
43	2002/11/22	01:34:07.4	35.67	36.12	03.8	4.8	–	066	60	−175	336	90	−035	11	Kensaba
44	2003/02/26	03:07:31.0	35.61	36.02	03.8	5.0	–	121	40	−050	256	60	−115	11	
45	2003/03/25	18:32:23.3	35.28	36.06	03.8	4.5	–	356	90	−125	266	35	000	9	Banyas
46	2003/05/20	03:27:34.6	36.04	36.59	08.5	4.0	–	336	90	−135	246	45	000	10	Al-Rouge
47	2003/07/13	17:02:10.0	35.65	36.11	03.8	3.8	–	071	50	−080	236	40	−100	11	Kensaba
48	2003/07/22	17:32:47.2	35.72	36.22	03.8	3.8	–	271	45	−105	111	50	−075	11	
49	2003/08/31	11:59:54.9	35.46	36.01	04.1	3.5	–	131	90	−120	041	30	000	12	

Appendix 2

Examples of the *P* first motion plots and the data. (*Take off according to Aki and Richards 1980.)

Motion plots	Station	Data from plots: Ray angle orientation Azimuth	Take-off *	*P* polarity
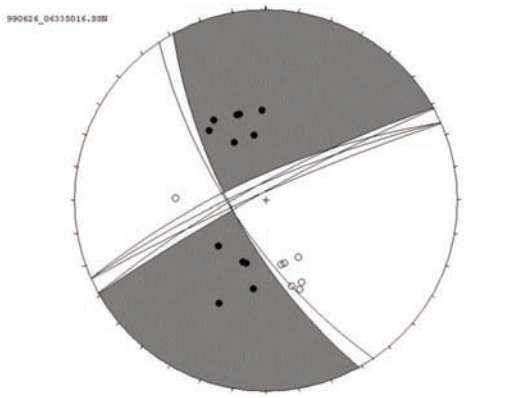	SLMH	20.2	148.4	+1
	JHLN	45.9	148.4	+1
	WHBV	17.1	148.4	+1
	KFRA	7.8	137.0	+1
	WRDH	343.2	137.0	−1
	BIDA	339.4	134.2	−1
	HWKV	24.3	125.8	+1
	SALA	151.5	148.4	+1
	BDRN	161.5	137.0	+1
	QASN	163.3	137.0	+1
	KOOC	141.1	137.0	+1
	MARH	147.1	134.2	+1
	RABV	90.9	137.0	−1
	DRWC	346.3	148.4	−1
	BTCH	343.3	148.4	−1
	ARNV	330.3	148.4	−1
	SLNF	336.3	137.0	−1
	TCHB	170.0	148.4	+1
	BARV	177.5	137.0	+1
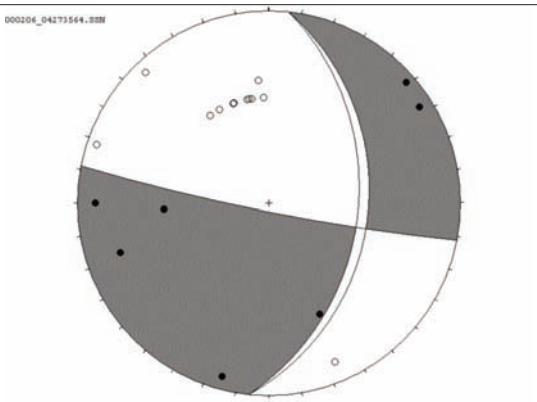	SLMH	49.0	87.4	+1
	JHLN	86.7	129.8	+1
	WHBV	57.7	85.4	+1
	KFRA	157.2	82.0	−1
	WRDH	251.6	74.7	+1
	BIDA	195.1	85.4	+1
	HWKV	175.2	121.6	−1
	ZLFV	151.9	129.8	−1
	SALA	160.9	129.8	−1
	BDRN	169.3	129.8	−1
	QASN	170.9	129.8	−1
	KOOC	160.3	129.8	−1
	MARH	168.2	129.8	−1
	RABV	146.1	129.8	−1
	DRWC	335.2	121.6	+1
	BTCH	316.4	85.5	−1
	ARNV	288.5	86.8	−1
	SLNF	270.0	82.8	+1
	BARV	177.3	129.8	−1
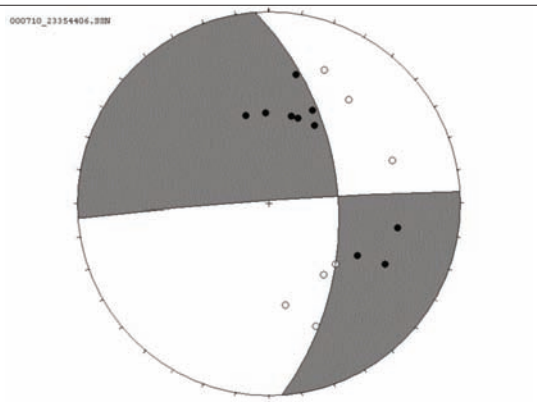	SLMH	350.6	130.8	−1
	WHBV	338.9	117.3	−1
	KFRA	297.5	117.3	+1
	WRDH	300.2	130.8	+1
	BIDA	280.6	117.3	+1
	HWKV	251.1	117.3	−1
	ZLFV	165.4	136.9	+1
	SALA	178.3	136.9	+1
	BDRN	199.2	136.9	+1
	QASN	205.4	130.8	+1
	KOOC	192.0	117.3	+1
	MARH	217.8	117.3	−1
	RABV	202.8	111.0	−1
	DRWC	322.1	136.9	−1
	BTCH	312.2	136.9	−1
	TCHB	194.8	136.9	+1
	BARV	210.8	136.9	+1
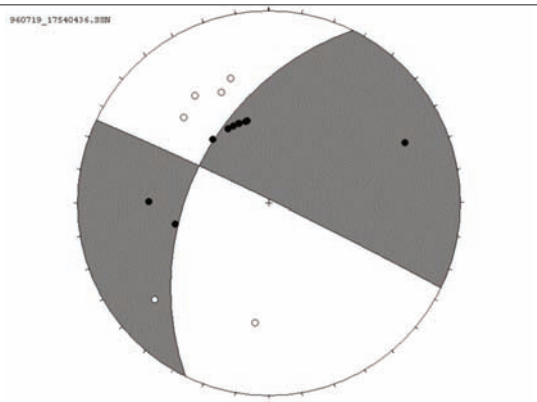	SLMH	77.4	134.3	+1
	WHBV	90.5	122.7	+1
	KFRA	135.1	122.7	−1
	WRDH	145.5	118.0	−1
	BIDA	156.7	122.7	−1
	BDRN	159.3	139.7	+1
	QASN	159.8	139.7	+1
	KOOC	151.3	139.7	+1
	MARH	155.2	139.7	+1
	RABV	138.3	139.7	+1
	DRWC	6.4	122.7	−1
	BTCH	49.9	108.8	−1
	ARNV	246.2	108.8	+1
	SLNF	162.9	118.0	−1
	TCHB	164.2	139.7	+1
	BARV	165.4	139.7	+1